A study of three-dimensional edge and corner problems using the neBEM solver

Supratik Mukhopadhyay *, Nayana Majumdar

INO Section, Saha Institute of Nuclear Physics, 1/AF, Sector 1, Bidhannagar, Kolkata 700064, WB, India

ABSTRACT

The previously reported neBEM solver has been used to solve electrostatic problems having three-dimensional edges and corners in the physical domain. Both rectangular and triangular elements have been used to discretize the geometries under study. In order to maintain very high level of precision, a library of C functions yielding exact values of potential and flux influences due to uniform surface distribution of singularities on flat triangular and rectangular elements has been developed and used. Here we present the exact expressions proposed for computing the influence of uniform singularity distributions on triangular elements and illustrate their accuracy. We then consider several problems of electrostatics containing edges and singularities of various orders including plates and cubes, and L-shaped conductors. We have tried to show that using the approach proposed in the earlier paper on neBEM and its present enhanced (through the inclusion of triangular elements) form, it is possible to obtain accurate estimates of integral features such as the capacitance of a given conductor and detailed ones such as the charge density distribution at the edges/corners without taking resort to any new or special formulation. Results obtained using neBEM have been compared extensively with both existing analytical and numerical results. The comparisons illustrate the accuracy, flexibility and robustness of the new approach quite comprehensively.

1. Introduction

One of the elegant methods for solving the Laplace/Poisson equations (normally an integral expression of the inverse square law) is to set up the boundary integral equations (BIE) which lead to the moderately popular boundary element method (BEM). In the forward collocation version of the BEM, surfaces of a given geometry are replaced by a distribution of point singularities such as source/dipole of unknown strengths. The strengths of these singularities are obtained through the satisfaction of a given set of boundary conditions that can be Dirichlet, Neumann or of the Robin type. The numerical implementation requires considerable care [1] because it involves evaluation of singular (weak, strong and hyper) integrals. Some of the notable two-dimensional (while all the devices are three-dimensional by definition, useful insight is often obtained by performing a two-dimensional analysis) and three-dimensional approaches used to evaluate the singular integrals are discussed in [1–7] and the references in these papers. It is well-understood that many of the difficulties in the available BEM solvers stem from the assumption of nodal concentration of singularities which leads to various mathematical difficulties and to the infamous numerical boundary layers [8,9,33] when the source is placed very close to the field point ([2] and Refs. [4–6] therein). While mathematical singularities (that occur when the source and field points coincide) have been shown to be artifacts, several techniques have been used to remove difficulties related to physical or geometrical singularities (that occur when boundaries are degenerate, i.e., geometrically singular, or due to a jump in boundary conditions) such as Gaussian quadrature integration, mapping techniques for regularization, bicubic transformation, nonlinear transformation and dual BEM techniques [8]. The last technique seems to be a popular one and capable of dealing with a relatively wide range of similar problems.

Departing from the approaches mentioned in the above references and many more to be mentioned below, we had shown in an earlier paper [10] that many of these problems can be eliminated or reduced if we adopt a new paradigm in which the elements are endowed with singularities distributed on them, rather than assuming the singularities to be concentrated at specific nodal points. Despite a large body of literature, closed form analytic expressions for computing the effects of distributed singularities are rare [11,12], complicated to implement and, often, valid only for special cases [13–15]. For example, in [11], the integration of the Green function to compute the influence of a

* Corresponding author.
E-mail addresses: supratik.mukhopadhyay@saha.ac.in (S. Mukhopadhyay), nayana.majumdar@saha.ac.in (N. Majumdar).

constant source distribution is modified to an "n-plane" integration. The evaluation of this integration involves co-ordinate transformations and the resulting expressions are rather complicated. In [12], the Gauss–Bonnet concept is used in which the panel is projected onto a unit sphere and the solid angle is determined from the sum of the induced angles. The procedure and the resulting expressions are neither simple, nor easy to implement in a computer code. In fact, possibly due to these difficulties, these approaches have remained relatively unpopular and even in very recent papers it is maintained that for evaluating the influence due to source distributed on triangular elements in a general case, one must apply non-analytic procedures [14]. Thus, for solving realistic but difficult problems involving, for example, sharp edges and corners or thin or closely spaced elements, introduction of special formulations (usually involving fairly complicated mathematics, once again) becomes a necessity [8,16,33]. These drawbacks are some of the major reasons behind the relative unpopularity of the BEM despite its significant advantages over domain approaches such as the finite-difference and finite-element methods (FDM and FEM) while solving non-dissipative problems [17,18].

The Inverse Square Law Exact Solutions (ISLES) library developed in conjunction with the nearly exact BEM (neBEM) solver [10], in contrast, is capable of truly modeling the effect of distributed singularities precisely and, thus, is not limited by the proximity of other singular surfaces or their curvature or their size and aspect ratio. The library consists of analytic solutions for both potential and flux due to uniform distribution of singularity on flat rectangular and triangular elements. These close-form exact solutions, termed as *foundation expressions*, are in the form of algebraic expressions that are long but without complications and are fairly straight-forward to implement in a computer program. In deriving these foundation expressions, while the rectangular elements were allowed to be of any arbitrary size [10,19], the triangular element was restricted to be a right-angled triangle of arbitrary size [20–22]. Since any real geometry can be represented through elements of the above two types (or by the triangular type alone), this library has allowed us to develop the neBEM solver that is capable of solving three-dimensional potential problems involving arbitrary geometry. It may be noted here that any non-right-angled triangle can be easily decomposed into two right-angled triangles. Thus, the right-angled triangles considered here, in fact, can take care of any three-dimensional geometry.

A set of particularly difficult problems to be dealt with by BEM is one that contains corners and edges and, in this work, we will attempt to solve several problems belonging to this set. The perfectly conducting bodies studied here are unit square plate, L-shaped plate, cube, L-shaped volume and two rectangular plates meeting at various angles and creating an edge. Besides being interesting and difficult, these solutions can have significant applications in micro-electromechanical systems (MEMS), nano-devices, atomic force microscopy (AFM), electro-optical elements, micro-pattern gas detectors (MPGD) and many other disciplines in science and technology. For these problems, it is important to study integral features such as the capacitance of the conductors, as well as detailed features such as the charge density, potential and flux on various surfaces of these objects including regions close to the geometric singularities. While several approaches including FDM, FEM, BEM and its variants such as the surface charge method (SCM) and various implementations of the Monte-Carlo technique (often coupled with Kelvin transformation) have been used to study these problems, only the latter two approaches, namely, BEM and Monte-Carlo technique are found to possess the precision necessary to model the curiously difficult electrostatics with acceptable levels of accuracy [23]. The volume

discretization methods are known to be unsuitable because of the open nature of the problem and the inadequate representation of edge and corner singularities. Methods using Kelvin inversion (or quadratic inversion), although accurate, have been found incapable of handling planar problems. It may be noted here that despite the usefulness of two-dimensional analysis, there are an overwhelming number of problems that need to be addressed in three dimensions. As a result, several interesting approaches have been developed to analyze edge and corner related problems in complete three dimensions, without even the assumption of axial symmetry. In order to maintain applicability in the most general scenarios, in this work we will deal with the problems of edge and corner as truly three-dimensional objects even when comparing the results with two-dimensional analytic ones.

The problem of estimation of capacitance of square plate and cube raised to unit volt has been studied by an especially large number of workers using entirely different approaches. In fact, these have been considered to be some of the major unsolved problems of electrostatics, of which a solution is said to have been given by Dirichlet and subsequently lost. One of the more popular numerical approaches used to explore these problems is the BEM/SCM [13,24–28]. Some of the solution attempts are more than a century old and yielded quite acceptable results. The later studies [13,27,28] used the mesh refinement technique and extrapolation of N (the number of elements used to discretize a given body) to infinity in order to arrive at more precise estimates of the capacitance. In order to carry out this extrapolation, uniform charge density scenario has been maintained so that the form of charge distribution on individual segments becomes irrelevant. According to [28], it is justified to use uniform charge density on individual elements because increase in complexity through the use of non-uniform charge density ultimately does not lead to computational advantage. In [28], the author mentions that for the cube, the element sizes are made such that the charge on each element remains approximately a constant (independent of its distance from an edge) since this arrangement is found to give the most accurate results.

The problem of estimation of the order of singularities at edges and corners of different nature is strongly coupled with the problem of estimation of integral properties such as the capacitance of conductors of various shapes. Thus, this problem, which also has importance in relation to other areas of science and technology as discussed earlier, has attracted the attention of a large number of workers as well. Here, fortunately, some analysis has been possible using purely theoretical tools [29,30], at least for two-dimensional cases. In [31], the authors used a singular perturbation technique to obtain the singularity index at inside and outside corners of a sectorial conducting plate. Similarly, corner singularity exponents were numerically obtained in [28]. According to [32], it was possible to achieve accuracy of one in million through the use of FEM approximations for both electrodes and surface charge density, in addition to proper handling of edge and corner singularities. In this investigation, the Fichera's theorem was used to correctly describe the peculiarities of surface charge density behavior in the vicinity of the electrode ribs and tips.

According to another recent work [33], low-order polynomials used to represent the corners and edges lead to errors in estimation of the derivatives of the potential, and that is the crux of the problem. Despite its advantages (no prior knowledge of singular elements and the order of singularity is necessary) and good convergence characteristics, the mesh refinement approach has been mentioned to be less accurate than two other methods, namely, (1) singular elements, and (2) singular functions. Among these, beforehand knowledge of the location and behavior of the singularity in terms of the order of singularity is required for (1).

The singular function approach (2) performs the best since it uses both the above and also information on singularity profile (corresponding to the eigenvalues and eigenvectors of the given geometry). Unfortunately, this approach requires complex formulation and is generally restricted to two-dimensional. Since the singular element approach uses the location information and only the order of the singularity, it is more versatile and popular. Thus, [33] implements the method of singular elements in three dimensions while attempting to use proper shape function/ interpolation function to model correct singular behavior at corners and edges. It is shown that singular elements are needed to accurately capture the behavior at singular regions, such as sharp corners and edges, where standard elements fail to give an accurate result. Unfortunately, singular elements must be defined before it is possible to apply either the singular function or the singular element approach. This is a non-trivial task since for a realistic device, there can easily be thousands, if not millions, of elements involved. According to [34], the manual classification of boundary elements based on their singularity conditions is an immensely laborious task if not outright impractical. In [34], the authors developed an algorithm to extract the regions where singularity arises by querying the geometric model for convex edges based on geometric information of the model. The associated nodes of the boundary elements on these edges were then retrieved and categorized according to different types of singularity configuration. The algorithm developed was implemented in the PATRAN command language (PCL) on the MSC/PATRAN platform [35] which is an industry standard finite-element pre- and post-processor allowing a high degree of customization. In order to determine the order of singularity, two-dimensional results have been used directly [29,36] for edges under the assumption that the point lies sufficiently far from any corner. In fact, in [34], any point other than the vertices has been considered to be far enough. This approach is quite unlikely to be very accurate, especially when the dimensions of the devices are small enough so that no point may even be considered to be far enough. Later, while discussing the results obtained using our proposed approach, we will return to this issue again. A study on the effect of bias ratio (a ratio of the largest element length to the smallest element length, similar to *r*-mesh refinement) has led the authors [33] to state that while for normal elements this ratio should be around 4:1 for a given problem, the singular element approach works better with lower bias ratio.

Besides the above procedures to identify the singular elements and their orders, attempts have also been made to place nodes at optimal positions while solving problems involving edges and corners. For example, in fracture mechanics [37], for handling singularities of the order 0.5, mid-side nodes in quadratic elements are normally shifted to quarter point positions. Several other techniques such as least square, constrained displacement of side nodes adjacent to a crack-tip [38] have also been used to find the optimum position of the mid-side nodes for handling singularities of other orders. In [39], the authors have subsequently shown that this approach of shifting mid-side nodes is likely to produce singularities of order 0.5 only and it is not suitable to impose arbitrary singularity in isoparametric elements by simply shifting side nodes to assumed positions.

In addition to BEM approaches, work has also been carried out using radically different approaches, for example, the Monte-Carlo methods. An impressive array of work exists providing very accurate estimates of capacitance and variation of charge density near edges and corners [23,40–43,45,46]. According to [23], the use of BEM introduces unnatural estimate of the charge density distribution—not for shapes with smooth contours (disks or spheres), but for plates and cubes. It has been mentioned that the situation is worst for the corner singularities of plates in which

case there are no other surfaces present (as in a cube) to weaken the order of singularity at the corner. We will discuss this issue when results for square plates are presented below. The other point is that the BEM cannot satisfy the boundary conditions at or, at least, close to the edge because, the collocation points in BEM do not match the boundary of the device. In fact, it is mentioned that the solutions become unstable when the collocation points are shifted away from the centroid of the elements. This notion, as mentioned in the earlier paragraph, is not without counterexamples. Moreover, this is a point that we plan to take up in a future communication where we hope to illustrate that for the proposed formulation, shifting the collocation points to non-centroid locations does not lead to numerical instabilities. In addition, the approach of extrapolating capacitance has been criticized on the ground that they do not match for different amounts of shift. It has been mentioned that no formal error analysis exists for methods other than FDM and the extrapolation is purely empirical in nature. It has been observed that the apparent high accuracy may be illusory in nature and citing [47], it has been emphasized that situation can become even worse by attempting extrapolation of results obtained using non-equivalent meshes.

By developing a model that incorporates the truly distributed nature of sources/doublets/vortices on surfaces of three-dimensional geometries, we have recently shown [10,19,22] that it is possible to use the same formulation for studying a very wide range of problems (multi-scale, involving multiple layers of dielectric materials) governed by the Poisson's equation. Recently, we have extended the new formulation with the capability of including triangular elements as an option for discretizing arbitrary three-dimensional bodies [20,21]. Here, we present the expressions to evaluate the exact values of potential and fluxes at any arbitrary point due to uniform singularity distributed on right-angled triangular element. These expressions have been included as additional functions of the ISLES library and subsequently used in the neBEM solver in the manner usual to, probably, most of the BEM solvers available. Besides presenting the expressions, we have also shown results to illustrate the accuracy of the expressions under various circumstances.

In this report, we have presented studies on the electrostatic configuration of several three-dimensional bodies, all of which contain corners and/or edges. The classic benchmark problems of estimating the capacitance of a unit square plate and unit cube raised to unit volt have been addressed. Electrostatics of generic shapes such as L-shaped plate and L-shaped three-dimensional conductors has also been analyzed. In all the above cases, the order of the singularity distribution near the edges and corners has been estimated in addition to estimating the capacitance of the conductors themselves. The singularity distributions obtained have been compared with theoretical and numerical studies carried out by earlier workers. The variation of the singularity along an edge between two corners at its ends has been studied, probably for the first time. Finally, the well-known problem of electrostatic configuration of two planes intersecting at different angles has been addressed. The two-dimensional counter-part of this problem is known to have analytic solution and has even been discussed in several textbooks on electromagnetics [29,30]. Although accessible analytically, this problem seems to have been rarely solved using numerical techniques [48]. This benchmark problem is known to be a difficult one and, in order to test the proposed approach under difficult circumstances, we have computed electrostatic properties of a three-dimensional analogue of this problem close to the point of intersection for a very wide range of angle of intersection. Following the above studies, we have come to the conclusion that the proposed approach is capable of solving critical multi-scale problems governed by the

Poisson's equation in a rather straight-forward manner. While higher bit accuracy, improved evaluation of transcendental functions, adaptive mesh generation and parallelization is expected to be of significant help, no special mathematical treatment or new formulation has been found to be necessary to deal with problems involving corners/edges and extremely closely spaced surfaces.

According to [23], using BEM, it is difficult to obtain physically consistent results close to these geometric singularities. Wild variations in the magnitude of the charge density have been observed with the change in the degree of discretization, the reason once again being associated with the nodal model of singularities. In contrast, using neBEM, we have obtained very smooth variation close to corner. Presence of oscillations seemingly acceptable to [23] has not occurred. In fact, oscillations close to edges and corners considered in this work seem to indicate numerical inaccuracy and have been treated accordingly. In addition to the shape, the magnitudes of the charge density have been found to be consistently converging to physically realistic values. These results clearly indicate that since the foundation expressions of the solver are exact, it is possible to find the potential and flux accurately in the complete physical domain, including the critical near-field domain using neBEM. In addition, since the singularities are no longer assumed to be nodal and we have the exact expressions for potential and flux throughout the physical domain, the boundary conditions no longer need to be satisfied at *special* collocation points such as the centroid of an element. Although consequences of this considerable advantage are still under study, it is expected that this feature will allow neBEM to yield even more accurate estimates for problems involving corners and edges since it should be possible to generate an over-determined system of equations by placing extra collocation points near the edges/corners. This will also allow the method to satisfy the boundary conditions of a given geometry at its true boundaries.

It should be noted here that the exact expressions for triangular elements consist of a significantly larger number of mathematical operations than those for rectangular elements presented in [10]. Thus, for any solver based on the ISLES library, it is more economical to use a mixed mesh of rectangular and triangular elements using rectangular elements as much as possible.

2. Governing equations and exact solutions

In the following discussions, we will concentrate on the electrostatics of conducting geometries governed by the Poisson's equation. Using BEM approach, the Poisson's equation for electrostatic potential

$$\nabla^2 \phi(\vec{r}) = -\rho(\vec{r})/\varepsilon_0$$

can be solved to obtain the distribution of charges which leads to a given potential configuration. For a point charge q at $\vec{r}'$ in three-dimensional space, the potential $\phi(\vec{r})$ at $\vec{r}$ is known to be

$$\phi(\vec{r}) = \frac{q}{4\pi\varepsilon_0 |\vec{r} - \vec{r}'|}$$

For a general charge distribution with charge density $\rho(\vec{r}')$, superposition holds and results in

$$\phi(\vec{r}) = \int \frac{\rho(\vec{r}')\,\mathrm{d}v'}{4\pi\varepsilon_0 |\vec{r} - \vec{r}'|} = \int G(\vec{r}, \vec{r}')\rho(\vec{r}')\,\mathrm{d}v' \tag{1}$$

where

$$G(\vec{r}, \vec{r}') = \frac{1}{4\pi\varepsilon_0 |\vec{r} - \vec{r}'|}$$

is the free space Green's function for the Laplace operator in three dimensions with ε_0, the permittivity of free space. Similarly, the field for a general charge distribution can be written as

$$\vec{E}(\vec{r}) = -\nabla\phi$$

leading to

$$\vec{E}(\vec{r}) = -\nabla\left(\int G(\vec{r}, \vec{r}')\rho(\vec{r}')\,\mathrm{d}v' \right)$$

and, finally to,

$$\vec{E}(\vec{r}) = \int \frac{\rho(\vec{r}')(\vec{r} - \vec{r}')\,\mathrm{d}v'}{4\pi\varepsilon_0 |\vec{r} - \vec{r}'|^3} \tag{2}$$

The charge distribution can be obtained from Eq. (1) or (2) by satisfying the boundary conditions at collocation points known either in the form of potential (Dirichlet) or flux (Neumann) or a mixture of these two (Mixed/Robin) on material boundaries/surfaces present in the domain.

Considering the Dirichlet problem only at present (for ease of discussion), the following integral equation of the first kind can be set up:

$$\phi(\vec{r}) = \int_{vol} G(\vec{r}, \vec{r}')\rho(\vec{r}')\,\mathrm{d}v' \tag{3}$$

In the above equation, $\phi(\vec{r})$ is the potential at a point $\vec{r}$ in space and $\rho(\vec{r}')$ is the charge density at an infinitesimally small volume $\mathrm{d}v'$ placed at $\vec{r}'$. The problem is, generally, to find $\rho(\vec{r}')$ as a function of space resulting the known distribution of $\phi(\vec{r})$. Once the charge distribution on the boundaries and all the surfaces is known, potential and field at any point in the computational domain can be obtained using the same Eq. (3) and its derivative.

The primary step of the BEM technique is to discretize the boundaries and surfaces of a given problem. The elements resulting out of the discretization process are normally rectangular or triangular though elements of other shapes are also used. Elements of triangular shape can be used to model geometries of any variety and, thus, is one of the most commonly used in many approaches of numerical simulation including FEM and BEM. In the collocation approach, the next step is to find out charge distribution on the elements that satisfies Eq. (3) following the given boundary conditions. The charge distribution is normally represented in terms of known basis functions with unknown coefficients. For example, in zeroth order formulations using constant basis function, which is also the most popular one among all the BEM formulations because of a good optimization between accuracy and computational complexity, the charge distribution on each element is assumed to be uniform and equivalent to a point charge located at the centroid of the element. This is the method that is referred to as the *usual BEM* in the rest of the paper. However, diverse varieties of basis function have been exercised to develop many more BEM formulations in order to represent the charge distribution on an element more efficiently so as to enhance the accuracy of the method. Since the potentials on the surface elements are known from the given potential configuration, Eq. (3) can be used to generate algebraic expressions relating unknown charge densities and potentials at the centroid of the elements. One unique equation can be obtained for each centroid considering influences of all other elements including self-influence and, thus, the same number of equations can be generated as there are unknowns. In matrix form, the resulting system of simultaneous linear algebraic set of equations can be written as follows:

$$\mathbf{K} \cdot \rho = \phi \tag{4}$$

where $\mathbf{K}$ is the matrix consisting of influences among the elements due to unit charge density on each of them, ρ represents

a column vector of unknown charge densities at centroids of the elements and ϕ represents known values of potentials at the centroids of these elements. Each element of this influence coefficient or capacity coefficient matrix, **K** is a direct evaluation of an equation similar to Eq. (1) or (2) which represents the effect of a single element on a boundary/surface (obtained through discretization) on a point where a boundary condition of the given problem is known. While, in general, this should necessitate an integration of the Green's function over the area of the element, this integration is avoided in most of the BEM solvers through the assumption of nodal concentration of singularities with known basis function. The construction of the matrix implies that its diagonal elements are dominant through the presence of the Coulomb-type singularity in the kernel. This singularity has been shown to make the solutions well-defined in the class of rather smooth functions [32]. Since the right-hand side of (4) is known, in principle, it is possible to solve the system of algebraic equations and obtain surface charge density on each of the element used to describe the conducting surfaces of the detector following:

$$\rho = \mathbf{K}^{-1} \cdot \phi$$

Once the charge density distribution is obtained, Eqs. (1) and (2) can be used to obtain both potential and field at any point in the computational domain.

Despite the elegance of formulation, the usual BEM suffers from several drawbacks that have resulted in its relative lack of popularity. Two of the most important ones can be mentioned as follows. (i) It is assumed that a surface distribution of charge density on an element can be represented by a nodal arrangement based on a chosen basis function. (ii) It is assumed that the satisfaction of the boundary condition at a predetermined point (or, through the use of known shape functions) is equivalent to satisfying the same on the whole element in a distributed manner. The former assumption leads to infamous numerical boundary layer [2,8,9,33] due to which the near-field solution in regions close to an element becomes erroneous. Thus the estimation of potential and field in near-field region close to the boundaries and surfaces by usual BEM is found to be inaccurate. This also leads to complications in solving problems involving closely spaced surfaces such as degenerate surfaces, edges, corners and other geometrical singularities. The degenerate surface refers to a boundary, two portions of which approach each other such that the exterior region between the two portions becomes infinitely thin. It is well known that the coincidence of two boundaries gives rise to an ill-conditioned problem. A number of special formulations has been developed to cope up with these problems but, unfortunately, most of these formulations are effective in a rather small subset of problems related to potential and field that are usually faced in reality.

This problem has been resolved to a great extent through the development of the neBEM solver that uses *exact integration* of the Green's function and its derivative in its formulation. These integrations for rectangular and triangular elements having uniform charge density have been obtained as closed-form analytic expressions using symbolic mathematics [10]. Thus they account for truly distributed nature of charge density on a given element. Besides the fundamental change in the way the influence coefficient matrix is computed and the foundation expressions used for evaluating potential and field at any point after the charge density vector is solved for, most of the other features of neBEM are similar to any other BEM solver.

The expression for potential and flux at a point (X, Y, Z) in free space due to uniform source distributed on a rectangular flat surface having corners situated at (x_1, z_1) and (x_2, z_2) has been
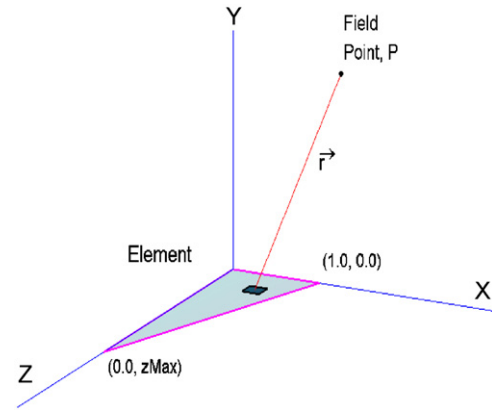

Fig. 1. Right-angled triangular element with x-length 1 and an arbitrary z-length, z_M; P is the point where the influence (potential and flux) is being computed.

presented, validated and used in [10,19] and, thus, is not being repeated here.

Here, we present the exact expressions necessary to compute the potential and flux due to a right-angled triangular element of arbitrary size, as shown in Fig. 1. It may be noted here that the length in the X direction has been normalized, while that in the Z direction has been allowed to be of any arbitrary magnitude, z_M. From the figure, it is easy to see that in order to find out the influence due to triangular element, we have imposed another restriction, namely, the necessity that the X- and Z-axes coincide with the perpendicular sides of the right-angled triangle. Both these restrictions are trivial and can be taken care of by carrying out suitable scaling and appropriate vector transformations. It may be noted here that closed-form expressions for the influence of rectangular and triangular elements having uniform singularity distributions have been previously presented in [12,13]. However, in these works, the expressions presented are quite complicated and difficult to implement. In [10] and in the present work, the expressions we have presented are lengthy, but completely straight-forward. As a result, the implementation issues of the present expressions, in terms of the development of the ISLES library and the neBEM solver, are managed quite easily. It is easy to show that the influence (potential) at a point $P(X, Y, Z)$ due to uniform source distributed on a right-angled triangular element as depicted in Fig. 1 can be represented as a multiple of

$$\Phi(X, Y, Z) = \int_0^1 \int_0^{z(x)} \frac{\mathrm{d}z\,\mathrm{d}x}{\sqrt{(X-x)^2 + Y^2 + (Z-z)^2}} \tag{5}$$

in which we have assumed that $x_1 = 0$, $z_1 = 0$, $x_2 = 1$ and $z_2 = z_M$, as shown in the geometry of the triangular element. The closed-form expression for the potential has been obtained using symbolic integration [49] which was subsequently simplified through substantial effort. It is found to be significantly more complicated in comparison to the expression for rectangular elements presented in [10] and can be written as

$$
\begin{aligned}
\Phi = \frac{1}{2}\Big(& (z_M Y^2 - XG)(LP_1 + LM_1 - LP_2 - LM_2) \\
& + \mathrm{i}|Y|(z_M X + G)(LP_1 - LM_1 - LP_2 + LM_2) \\
& - S_1 X\left(\tanh^{-1}\left(\frac{R_1 + \mathrm{i}I_1}{D_{11}|Z|}\right) + \tanh^{-1}\left(\frac{R_1 - \mathrm{i}I_1}{D_{11}|Z|}\right)\right. \\
& \left. - \tanh^{-1}\left(\frac{R_1 + \mathrm{i}I_2}{D_{21}|Z|}\right) - \tanh^{-1}\left(\frac{R_1 - \mathrm{i}I_2}{D_{21}|Z|}\right)\right)
\end{aligned}
$$

$$+ iS_1|Y|\left(\tanh^{-1}\left(\frac{R_1+iI_1}{D_{11}|Z|}\right) - \tanh^{-1}\left(\frac{R_1-iI_1}{D_{11}|Z|}\right)\right.$$
$$\left. -\tanh^{-1}\left(\frac{R_1+iI_2}{D_{21}|Z|}\right) + \tanh^{-1}\left(\frac{R_1-iI_2}{D_{21}|Z|}\right)\right)$$
$$+ \frac{2G}{\sqrt{1+z_M^2}}\log\left(\frac{\sqrt{1+z_M^2}D_{12}-E_1}{\sqrt{1+z_M^2}D_{21}-E_2}\right)$$
$$+ 2Z\log\left(\frac{D_{21}-X+1}{D_{11}-X}\right)\Bigg) + C \tag{6}$$

where

$$D_{11} = \sqrt{(X-x_1)^2+Y^2+(Z-z_1)^2}$$
$$D_{12} = \sqrt{(X-x_1)^2+Y^2+(Z-z_2)^2}$$

$$D_{21} = \sqrt{(X-x_2)^2+Y^2+(Z-z_1)^2}$$
$$I_1 = (X-x_1)|Y|, \quad I_2 = (X-x_2)|Y|$$

$$S_1 = \text{sign}(z_1-Z), \quad R_1 = Y^2+(Z-z_1)^2$$

$$E_1 = (X+z_M^2-z_MZ), \quad E_2 = (X-1-z_MZ)$$

$$G = z_M(X-1)+Z, \quad H_1 = Y^2+G(Z-z_M)$$
$$H_2 = Y^2+GZ$$

$$LP_1 = \frac{1}{G-iz_M|Y|}\log\left(\frac{(H_1+GD_{12})+i|Y|(E_1-z_MD_{12})}{-X+i|Y|}\right)$$

$$LM_1 = \frac{1}{G+iz_M|Y|}\log\left(\frac{(H_1+GD_{12})-i|Y|(E_1-z_MD_{12})}{-X-i|Y|}\right)$$

$$LP_2 = \frac{1}{G-iz_M|Y|}\log\left(\frac{(H_2+GD_{21})+i|Y|(E_2-z_MD_{21})}{1-X+i|Y|}\right)$$

$$LM_2 = \frac{1}{G+iz_M|Y|}\log\left(\frac{(H_2+GD_{21})-i|Y|(E_2-z_MD_{21})}{1-X-i|Y|}\right)$$

and C denotes a constant of integration.

Similarly, the flux components due to the above singularity distribution can also be represented through closed-form expressions as shown below:

$$F_x = -\frac{\partial\Phi}{\partial x} = \frac{1}{2}\Bigg((G)(LP_1+LM_1-LP_2-LM_2)$$
$$- i|Y|(z_M)(LP_1-LM_1-LP_2+LM_2)$$
$$+ S_1\left(\tanh^{-1}\left(\frac{R_1+iI_1}{D_{11}|Z|}\right) + \tanh^{-1}\left(\frac{R_1-iI_1}{D_{11}|Z|}\right)\right.$$
$$\left. - \tanh^{-1}\left(\frac{R_1+iI_2}{D_{21}|Z|}\right) - \tanh^{-1}\left(\frac{R_1-iI_2}{D_{21}|Z|}\right)\right)$$
$$+ \frac{2z_M}{\sqrt{1+z_M^2}}\log\left(\frac{\sqrt{1+z_M^2}D_{12}-E_1}{\sqrt{1+z_M^2}D_{21}-E_2}\right)\Bigg) + C \tag{7}$$

$$F_y = -\frac{\partial\Phi}{\partial y} = \frac{-1}{2}\Bigg((2z_MY)(LP_1+LM_1-LP_2-LM_2)$$
$$+ i(Sn(Y)G)(LP_1-LM_1-LP_2+LM_2)$$
$$+ iS_1Sn(Y)\left(\tanh^{-1}\left(\frac{R_1+iI_1}{D_{11}|Z|}\right)\right.$$
$$- \tanh^{-1}\left(\frac{R_1-iI_1}{D_{11}|Z|}\right) - \tanh^{-1}\left(\frac{R_1+iI_2}{D_{21}|Z|}\right)$$
$$\left. + \tanh^{-1}\left(\frac{R_1-iI_2}{D_{21}|Z|}\right)\right)\Bigg) + C \tag{8}$$

and,

$$F_z = -\frac{\partial\Phi}{\partial z} = \left(\frac{1}{\sqrt{1+z_M^2}}\log\left(\frac{\sqrt{1+z_M^2}D_{21}-E_2}{\sqrt{1+z_M^2}D_{12}-E_1}\right)\right.$$
$$\left. + \log\left(\frac{D_{11}-X}{D_{21}-X+1}\right)\right) + C \tag{9}$$

where $Sn(Y)$ implies the sign of the Y-coordinate and C indicates constants of integrations. It is to be noted that the constants of different integrations are not the same. In addition to being extremely useful in the mathematical modeling of physical processes governed by the inverse square laws, these expression are expected to be useful as benchmark expressions for other approximate formulations. Being exact and valid throughout the physical domain, they can be used to formulate versatile solvers to solve multi-scale multi-physics problems governed by the Laplace/Poisson equations involving Dirichlet, Neumann or Robin boundary conditions.

3. Results and discussions

3.1. Exact expressions

The expressions for the rectangular element have been validated in detail in [10]. Here, we present the results for triangular elements in fair detail. In Fig. 2, we have presented a comparison of potentials evaluated for a unit triangular element by using the exact expressions, as well as by using numerical quadrature of high accuracy. The two results are found to compare very well throughout. Note that contours have been obtained on the plane of the element, and thus, represents a rather critical situation. Similarly, Fig. 3 shows a comparison between the results obtained using closed-form expressions for flux and those obtained using numerical quadrature. The flux considered here is in the Y direction and is along a line beginning from $(-2,-2,-2)$ and ending at $(2,2,2)$. The comparison shows the commendable accuracy expected from closed-form expressions.
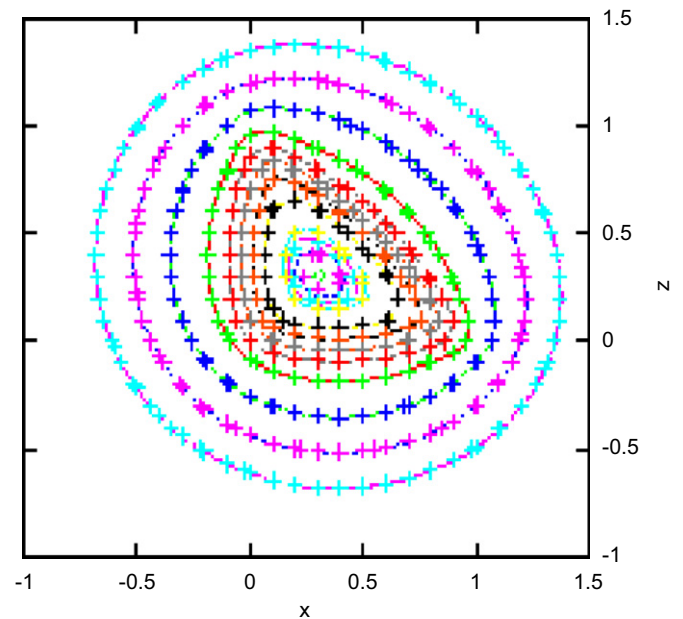

Fig. 2. Potential contours on a triangular element computed using exact expressions and by numerical quadrature.

In Figs. 4(a) and (b), the surface plots of potential on the element plane (XZ plane) and Y-flux on the XY plane have been presented from which the expected significant increase in potential and sharp change in the flux value on the element are observed. Thus, by using a small fraction of computational resources in comparison to those consumed in numerical quadratures, ISLES can compute the exact value of potential and flux for singularities distributed on triangular elements.

3.1.1. Near-field performance

In order to emphasize the accuracy of ISLES, we have considered the following severe situations in the near-field region in which it is observed that the quadratures can match the accuracy of ISLES only when a high degree of discretization is used. Note that in these cases, the value of z_M has been considered to be 10. In Fig. 5 we have presented the variation of potential along a line on the element surface running parallel to the Z-axis of the triangular element (see Fig. 1) and going through the centroid of the element. It is observed that results obtained using even a 100×100 quadrature are quite unacceptable. In fact, by zooming on to the image, it can be found that only the maximum discretization yields results that match closely to the exact solution. It may be noted here that the potential is a relatively easier property to compute. The difficulty of achieving accurate

flux estimates is illustrated in the two following figures. The variation of flux in the X-direction along the same line as used in Fig. 5 has been presented in Fig. 6. Similarly, variation of Y-flux along a diagonal line (beginning at $(-10, -10, -10)$ and ending at $(10, 10, 10)$ and piercing the element at the centroid) has been presented in Fig. 7. From these figures we see that the flux values obtained using the quadrature are always inaccurate even if the discretization is as high as 100×100. We also observe that the estimates are locally inaccurate despite the use of very high amount of discretization (200×200 or 500×500). Specifically, in the latter figure, even the highest discretization cannot match the exact values at the peak, while in the former only the highest one can correctly emulate the sharp change in the flux value. It is also heartening to note that the values from the quadrature using higher amount of discretization consistently converge towards the ISLES values.

3.1.2. Far-field performance

It is expected that beyond a certain distance, the effect of the singularity distribution can be considered to be the same as that of a centroidally concentrated singularity or a simple quadrature. The optimized amount of discretization to be used for the quadrature can be determined from a study of the speed of execution of each of the functions in the library and has been
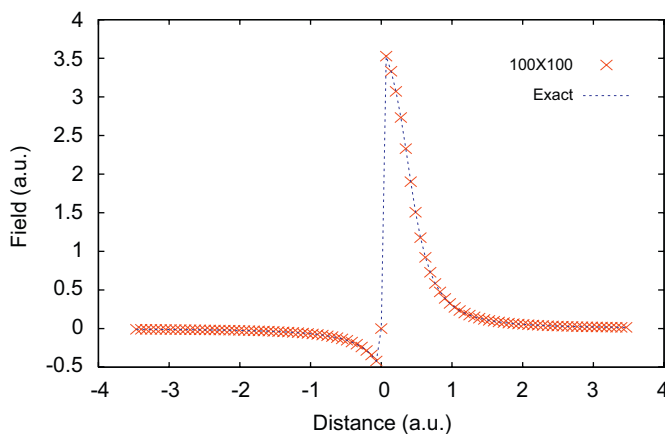

Fig. 3. Comparison of flux (in the Y direction) as computed by ISLES and numerical quadrature along a diagonal line.
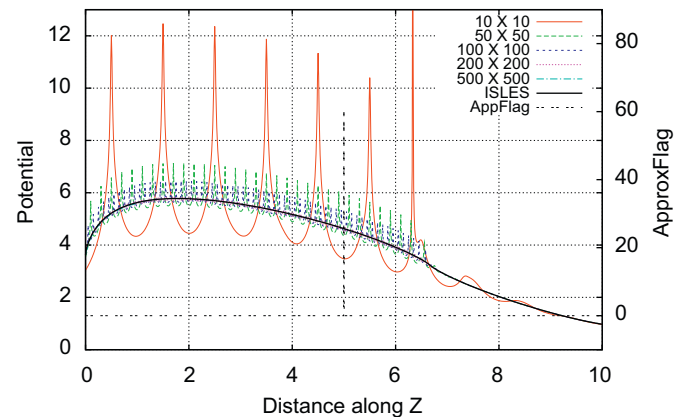

Fig. 5. Variation of potential along a centroidal line on the XZ plane parallel to the Z-axis for a triangular element: comparison among values obtained using the exact expressions and numerical quadratures.
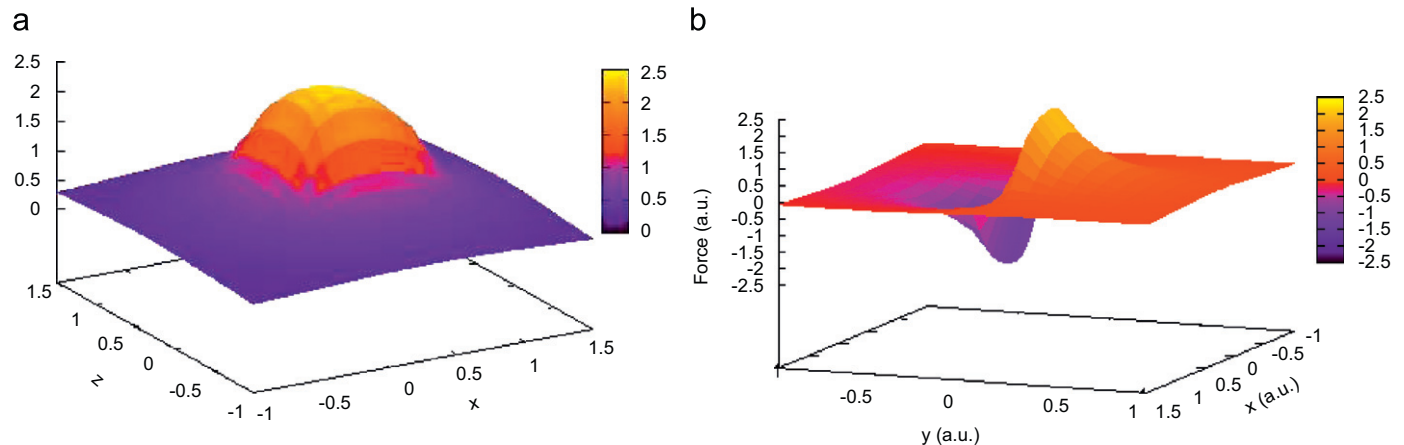

Fig. 4. (a) Potential surface due to a triangular source distribution on the element plane. (b) Flux (in the Y direction) surface due to a triangular source distribution on the XY plane at $Z = 0$.
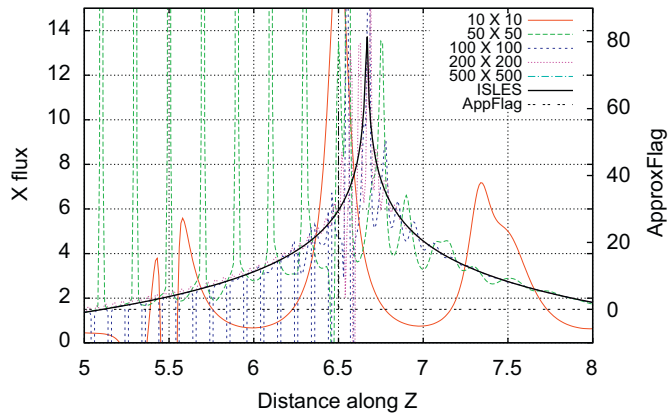
Fig. 6. Variation of flux in the *X* direction along a line on the *XZ* plane parallel to the *Z*-axis for a triangular element: comparison among values obtained using the exact expressions and numerical quadratures.
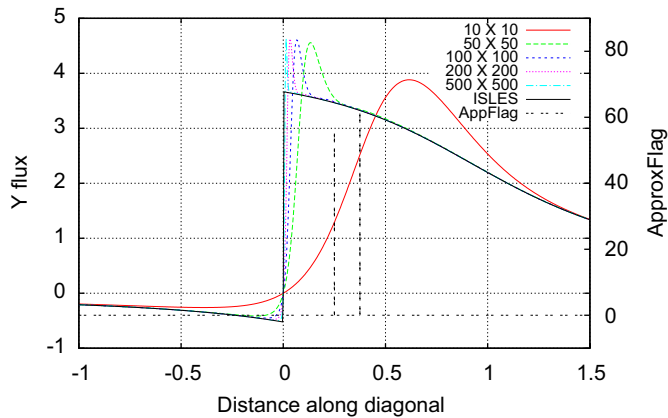

Fig. 8. Potential along a diagonal through the triangular element computed using exact, 100×100, 10×10 and usual BEM approach.

Fig. 7. Comparison of flux (in the *Y* direction) along a diagonal line piercing the triangular element at the centroid: comparison among values obtained using the exact expressions and numerical quadratures.
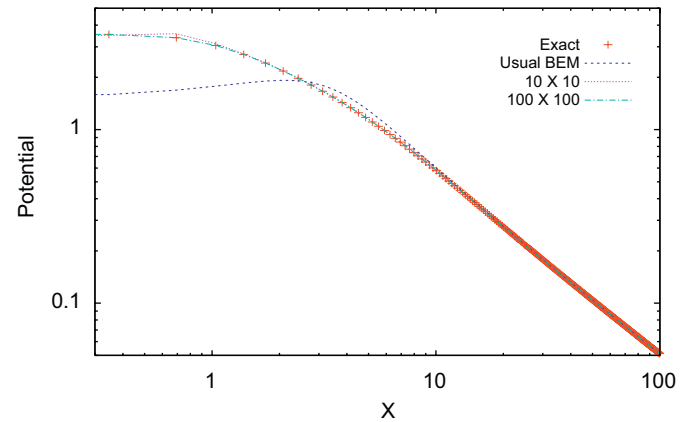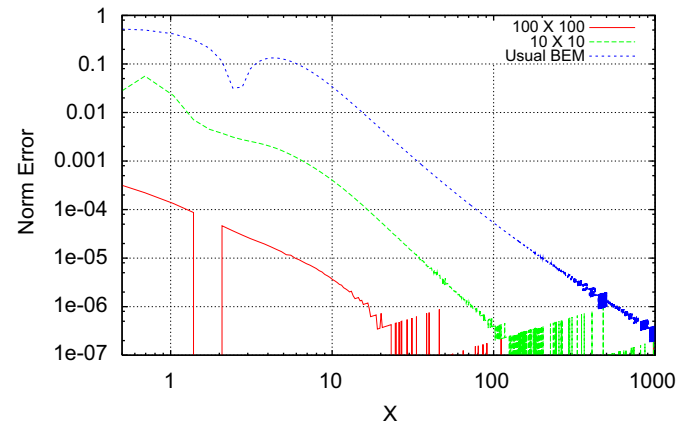

Fig. 9. Error along a diagonal through the triangular element computed using 100×100, 10×10 and usual BEM approach.

presented separately in a following sub-section. If we plan to replace the exact expressions by quadratures (in order to reduce the computational expenses, presumably) beyond a certain given distance, the quadrature should necessarily be efficient enough to justify the replacement. While standard but more elaborate algorithms similar to the fast multipole method (FMM) [50] along with the GMRES [51] matrix solver can lead to further of computational efficiency, the simple approach as outlined above can help in reducing a fair amount of computational effort. In the following, we present the results of numerical experiments that help us in determining the far-field performance of the exact expressions and quadratures of various degrees that, in turn, help us in choosing the more efficient approach for a desired level of accuracy.

In Fig. 8, we have presented potential values obtained using the exact approach, 100×100, 10×10 and no discretization, i.e., the usual BEM approximation while using the zeroth order piecewise uniform charge density assumption. The potentials are computed along a diagonal line running from $(-1000, -1000, -1000)$ to $(1000, 1000, 1000)$ which pierces a triangular element of $z_M = 10$. It can be seen that results obtained using the usual BEM approach yields inaccurate results as we move closer than distances of 10 units, while the 10×10 discretization yields acceptable results up to a distance of 1.0 unit. In order to visualize the errors incurred due to the use of quadratures, we have plotted Fig. 9 where the errors incurred (normalized with respect to the exact

value) have been plotted. From this figure we can conclude that for the given diagonal line, the error due to the usual BEM approximation falls below 1% if the distance is larger than 20 units while for the simple 10×10 discretization, it is 2 units. It may be mentioned here that along the axes the error turns out to be significantly more [10] and the limits need to be effectively doubled to achieve the accuracy for all cases possible. Thus, for achieving 1% accuracy, the usual BEM is satisfactory only if the distance of the influenced point is at least five times the longer side of an element. Note here that the error drops to 1 out of 10^6 as the distance becomes 50 times the longer side. Besides proving that the exact expressions work equally well in the near-field as well as the far-field, this fact justifies the usual BEM approach for much of the computational domain leading to substantial savings in computational expenses.

3.1.3. Comparison with multipole expressions

We also compared the value of potential with estimates for the barycenter and other field point values as obtained from [14,15], the expression having been slightly modified. At the barycenter, the expression given is exact, whereas, the multipole (monopole+quadrupole) expression is expected to be valid at any arbitrary location. The accuracy depends on the distance from the element as discussed in the papers, an approximate rule being that the accuracy is of the order of 10^{-4} when the distance of the field point from the barycenter of the triangle is more than

5.5 times the longer side of the right triangle. For points less distant than the mentioned value, the triangle needs to be further segmented. Consulting Fig. 9, we may note that along a diagonally intersecting line, the usual BEM achieves this accuracy only when the distance of a field point is 8 times the larger side. The 10×10 discretization is as good for a field point that is distant twice the longer side.

In Table 1, we show the values estimated at the barycenter by ISLES, analytic [14] and numerical quadrature of different discretizations. Triangular elements of different sizes have been used keeping the *x*-side always of unit length. It is interesting to note that the right triangle for which two perpendicular sides are of equal length, it is most difficult to obtain the precise value of potential using quadrature. In fact, with a discretization of 2000×2000, we obtained the value of 2.407462, while with 5000×5000 we obtained 2.407323.

In Fig. 10, results from the above multipole expansion are compared with those obtained using ISLES and numerical quadrature with different levels of discretization along a line passing from $(-10, -10, -10)$ to $(10, 10, 10)$, the range being reduced to a distance of -2 to $+2$ for ease of viewing. Similar comparison has been carried along a line parallel to the *X*-axis passing through the barycenter of the element and in the same plane as the element in Fig. 11. As indicated correctly in [14,15], the multipole expansion works fine at distances far enough. At close distances, only the ISLES results are acceptable. Other options exist in terms of further discretization. In that sense, both multipole expansion and numerical quadrature are likely to work but it may be difficult to decide on the required level of discretization *a priori*. Moreover, any advantage in terms of computational expenses may be lost due to the necessity of increased discretization.

3.1.4. Speed of execution

The time taken to compute the potential and flux is an important parameter related to the overall computational efficiency of

Table 1
Comparison of estimated potential by ISLES, analytic and various quadratures

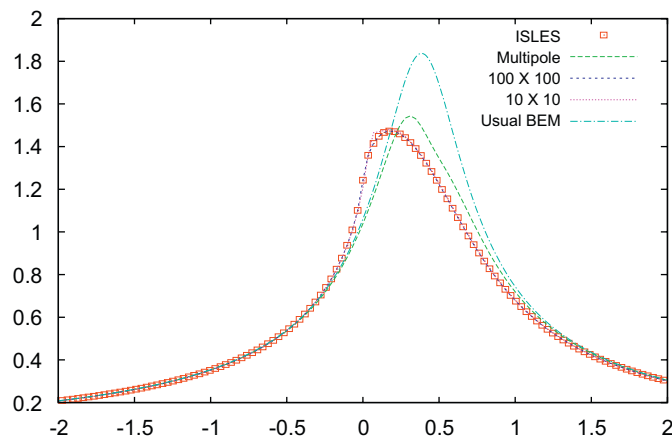| z_M	ISLES	Analytic [14]	10×10	100×100	500×500
0.1	0.545069	0.545069	0.5410382	0.5450810	0.5450695
1.0	2.407320	2.407320	2.460945	2.411947	2.408161
10.0	5.450690	5.450690	5.257222	5.450847	5.450696

Fig. 10. Potential along a diagonal through the triangular element computed using ISLES, multipole expansion, 100×100, 100×10 and usual BEM approach.
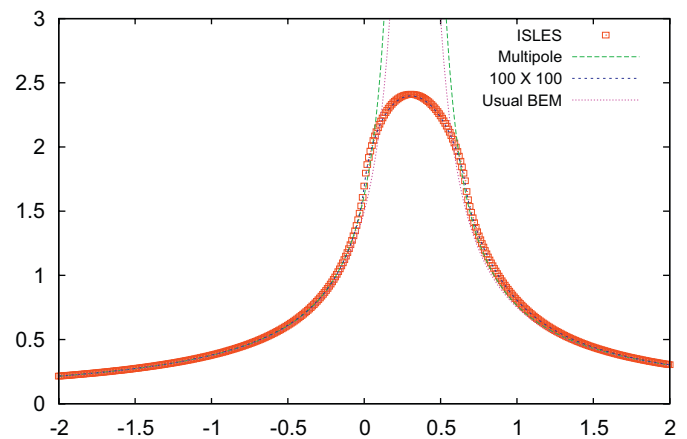

Fig. 11. Potential along a line parallel to *X* through the centroid of a triangular element computed using ISLES, multipole expansion, 100×100, 10×10 and usual BEM approach.

the codes. This is true despite the fact that, in a typical simulation, the time taken to solve the system of algebraic equation is far greater than the time taken to build the influence coefficient matrix and post-processing. Moreover, the amount of time taken to solve the system of equations tend to increase at a greater rate than the time taken to complete the other two. Thus, in fact, evaluation of longer expressions in the pre- and post-processing phase should hardly influence the efficiency of a BEM solver adversely. Moreover, due to the enhanced accuracy of the proposed foundation expressions, it will be possible to use significantly less number of elements to represent a given device, ultimately leading to much faster execution for a required level of accuracy. It should be mentioned here that the time taken in each of these steps can vary to a significant amount depending on the algorithm of the solver. In the present case, the system of equations has been solved using lower upper decomposition using the well-known Crout's partial pivoting. Although this method is known to be very rugged and accurate, it is not efficient as far as number of arithmetic operations, and thus time, is concerned. It is also possible to reduce the time taken to pre-process (generation of mesh and creation of influence matrices), solve the system of algebraic equations and that for post-process (computation of potential, flux at required locations, estimation of other properties such as capacitance, force) by adopting faster algorithms, including those involving parallelization.

In order to optimize the time taken to generate the influence coefficient matrix and that to carry out the post-processing, we carried out a small numerical study to determine the amount of time taken to complete the various functions being used in ISLES, especially those being used to evaluate the exact expressions and those being used to carry out the quadratures. The results of the study (which was carried out using the linux system command *gprof*) have been presented in Table 2.

Note that the numbers presented in this table are representative and are likely to have statistical fluctuations. However, despite the fluctuations, it may be safely concluded that a quadrature having only 10×10 discretization is already consuming time that is comparable to that needed for exact evaluation. Thus, the exact expressions, despite their complexity, are extremely efficient in the near-field which can be considered at least as large as 0.5 times the larger side of a triangular element (refer to Fig. 9). In making this statement, we have assumed that the required accuracy for generating the influence coefficient matrix and subsequent potential and flux calculations is only 1%.

This may not be acceptable at all under many practical circumstances, in which case the near-field would imply a larger volume.

Some of the advantages of using the ISLES library, based on the presented foundation expressions, are mentioned below:

- For a given level of discretization, the estimates are more accurate.
- Effective efficiency of the solver improves, as a result.
- Large variation of length-scales, aspect ratios can be tackled.
- Thinness of members or nearness of surfaces does not pose any problem.
- Curvature has no detrimental effect on the solution.
- The boundary condition can be satisfied anywhere on the elements, i.e., points other than the centroidal points can be easily used, if necessary (for a corner problem, may be).
- The same formulation, library and solver is expected to work in majority of physical situations. As a result, the necessity for specialized formulations of BEM and associated complications can be greatly minimized.

3.2. Electrostatics of two- and three-dimensional bodies having corners and edges

3.2.1. Square plate and cube

The capacitance value estimated by the present method has been compared with very accurate results available in the literature (using BEM and other methods). The results obtained using the neBEM solver are found to be among the most accurate ones available till date as shown in Table 3. Note that we have neither invoked symmetry nor used extrapolation techniques to arrive at our result presented in the table. In addition, it may also be noted that the square plates are considered to be of zero thickness.

In Table 4, we compare potentials at the center and along an edge of the unit cube as obtained using neBEM with those from [32] in which the authors use analytical techniques to determine the order of singularity at the singular regions of a cube. From this table, we find that it has been possible for [32] to maintain accuracy of 10^{-6} in 1 for the potential values at the cube center, 10^{-3}–10^{-2} in 1 along an edge and 10^{-2} in 1 along edge but close to a vertex of the cube. For similar locations, results using neBEM indicate that an accuracy of 10^{-6} is maintained at the cube center, 10^{-3} at the edge and 10^{-2} on the edge but close to the vertex. Thus, the proposed approach has been able to achieve accuracy that is comparable to those achieved by [32] that uses the Fichera's theorem to ensure proper variation of singularities near edges and vertices. Interestingly, at critical locations near the cube vertex, results from neBEM are found to be better than [32] by a significant amount. We have been able to maintain this accuracy of 10^{-2} as close as up to 1 µm to the cube vertex which is extremely encouraging. Unfortunately, we have not been able to compare our results with other numerical results at distances less than a mm from the vertex. It is encouraging to note, however, that while for [32], the error is 4.8×10^{-3} when the evaluation

Table 2
Time taken to evaluate exact expression of ISLES, usual BEM and various quadratures

Method	ISLES	Usual BEM	10×10	100×100	500×500
Time for rectangular element	0.6 µs	25 ns	2 µs	400 µs	10 ms
Time for two triangular elements	0.8 µs	25 ns	2 µs	400 µs	10 ms

Table 3
Comparison of capacitance values

Reference	Method	Plate (pF)/4 $\pi\varepsilon_0$	Cube (pF)/4 $\pi\varepsilon_0$
[24,25]	SCM	0.3638	
[26]	SCM	0.362	0.6555
[52]	SCM	0.367	
[13]	Refined SCM and extrapolation	$0.3667894 \pm 1.1 \times 10^{-6}$	$0.6606747 \pm 5 \times 10^{-7}$
[27]	Refined BEM and extrapolation	$0.3667874 \pm 1 \times 10^{-7}$	$0.6606785 \pm 6 \times 10^{-7}$
[43]	Numerical path integration	0.36684	0.66069
[23]	Random walk	0.36 ± 0.01	$0.6606 \pm 1 \times 10^{-4}$
[45]	Random walk		$0.6606780 \pm 2.7 \times 10^{-7}$
[33]	Singular element		0.6606749
[28]	Refined BEM and extrapolation	$0.3667896 \pm 8 \times 10^{-7}$	$0.6606767 \pm 4 \times 10^{-6}$
[15]	Robin Hood and extrapolation		$0.6606786 \pm 8 \times 10^{-8}$
This work	neBEM	0.3667524	0.6606746

Table 4
Comparison of potential at the center and along an edge of a unit cube

X	Y	Z	Exact	[32]	Error in [32]	neBEM	Error in neBEM
0	0	0	1	0.999990	-1.0×10^{-5}	1.000001	1.0×10^{-6}
0.4	0.5	0.5	1	0.9996	-4.0×10^{-4}	0.9994362	-5.638×10^{-4}
0.45	0.5	0.5	1	0.99986	-1.4×10^{-4}	0.9995018	-4.982×10^{-4}
0.49	0.5	0.5	1	1.0013	1.3×10^{-3}	0.9991151	-8.849×10^{-4}
0.499	0.5	0.5	1	1.0048	4.8×10^{-3}	0.9987600	-1.24×10^{-3}
0.4999	0.5	0.5	1	–	–	0.9974398	-2.56×10^{-3}
0.49999	0.5	0.5	1	–	–	0.9951335	-4.8×10^{-3}
0.499999	0.5	0.5	1	–	–	0.9945964	-5.4×10^{-3}

Table 5
Comparison of estimation of order of singularity

Reference	Method	Plate corner	Plate edge	Cube vertex	Cube edge
[29]	Analytic		0.5		0.333
[31]	Numerical shooting	0.7034			
[53]	BEM			0.5468	
[44]	Walk on spheres	0.7034		0.5381/ 0.5458	
[28]	Surface charge	0.704		0.540	
[45]	Surface charge			0.558	0.333
[33]	Singular element			0.5475	
[23]	Random walk				
[32]	Fichera's theorem	0.7015		0.5454	
[46]	Walk on planes	0.7034		0.5457	
This work	neBEM	0.7068	0.4994	0.5539	0.332

point is 1 mm away from the vertex, neBEM commits an error of a similar amount only when the point is 10 μm away from the vertex. The error for neBEM becomes larger by a small amount (0.4×10^{-3}) only when the evaluation point is as close as a micron to the vertex.

Next, we consider the problem of determining charge density distribution at corners and edges of the above geometries. Problems of this nature are considered to be challenging for any numerical tool and especially so for the BEM approach. In Table 5, we have presented the estimates of the order of singularity at the vertex or the edge as done by methods as diverse as singular perturbation [31], BEM [28], last-passage and walk on spheres [44,45], application of Fichera's theorem [32], singular element approach [33] and the presented approach. From the table, it is clear that there is good agreement among all the methods. As in [28] properties on the element next to a corner or edge have been ignored while carrying out the least-square fits. Points were included in the fit as long as the maximum mismatch between the fitted line and the computed value was less than typically 1%, which also allows us to include points as long as they fall closely on a straight line. Following this approach, we could use values of singularities even up to 0.15 (for a plate or cube of unit side) from the relevant edge or corner while fitting the lines (see Fig. 13, as an example where we used both triangular and rectangular elements for discretizing a square plate and obtained a singularity index of 0.7057 and 0.7068, respectively). These can be compared to the facts that in [28], two points next to a corner were excluded, as well as all points at distances beyond 0.05 from a corner. However, the exact value of the index is, to a certain extent, dependent on the discretization and the details of the least-square fitting procedure. Thus, it may not be very prudent to attach great significance to the obtained values except noting that they agree with each other and also agree with the theoretical estimates, wherever available. Thus, it may be difficult to accurately ascertain the singularity index at an arbitrary corner or edge. This difficulty can lead to problems for methods that depend on beforehand knowledge of the order of singularity.

In the following study, we have presented estimates of charge density very close to the flat plate corner as obtained using neBEM. This has been carried out to investigate the objection raised against the BEM in [23] where the author states that severe oscillations in the charge densities are expected close to the corner and edge of plates because the BEM cannot correctly model the edge/corner of physical devices. Note that for this study, the boundary conditions have been satisfied at the centroids of each element although the neBEM has the capability of satisfying boundary conditions at locations other than the centroid. In Fig. 12, charge densities very close to the corner of
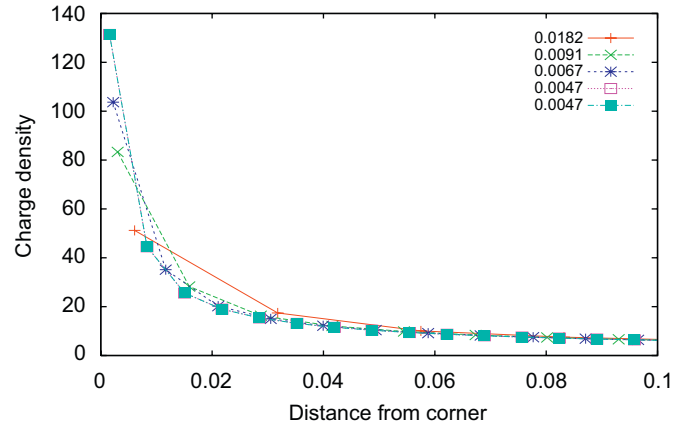

Fig. 12. Corner charge density estimated by neBEM using various sizes of triangular elements.
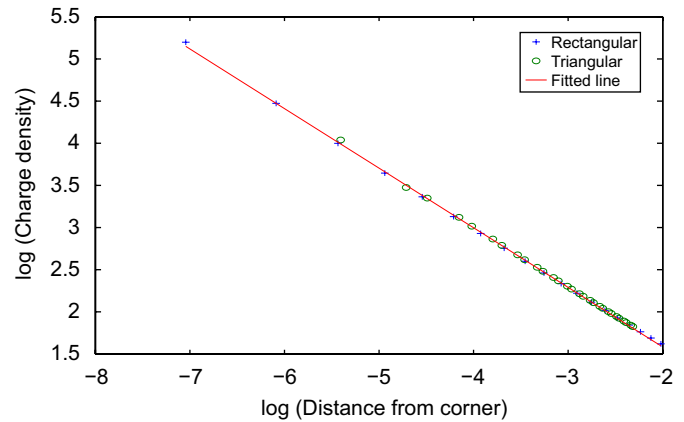

Fig. 13. Variation of charge density with increasing distance from the corner of the unit square plate and a least-square fitted straight line: slope of the fitted line is 0.7068.

the flat plate estimated by neBEM using various amounts of discretization have been presented. It can be seen that each curve follows the same general trend, does not suffer from any oscillation and is found to be converging to a single curve. This is true despite the fact that there has been almost an order of magnitude variation in the element lengths. Thus, we can safely conclude that the estimates obtained using neBEM do not suffer from the numerical instabilities mentioned in [23].

In Fig. 13, we present a least-square fitted straight line matching the charge density as obtained using the highest discretization in this study. Results using both triangular and rectangular elements are presented and it is found that the slope of the fitted line is 0.7057 when the elements are triangular, whereas, it is 0.7068 when we use rectangular elements. Both the values compare very well with both old and recent estimates of the order of singularity as shown in Table 5. The number of elements used to discretize the square plate is quite large in these computations. For example, in the case where the triangular elements are used, we have discretized the square plate into 6597 squares and divided each square into two right-angled triangles. The length of the side of each triangle varies from 0.005 units to 0.0267 units. In Fig. 14, we have shown how the slope of the fitted line changes along the edge of a square plate as we move away from a corner of a square plate. From the figure, it is apparent that the change in the singularity index along an edge of a square plate can be quite significant and only when we are in

reality close to the middle of the edge, the analytic value of 0.5 can be used with confidence for the order of singularity. This observation is significant especially for the singular element and singular function methods where prior knowledge of this parameter plays a crucial role in determining the accuracy of the solution.

3.2.2. L-shaped plate and volume

Despite being geometries of generic nature, these L-shaped geometries have received relatively less attention. Here, we have estimated the capacitance and orders of singularity at various important locations, e.g., inner and outer corners and compared these values with available numerical results. It should be 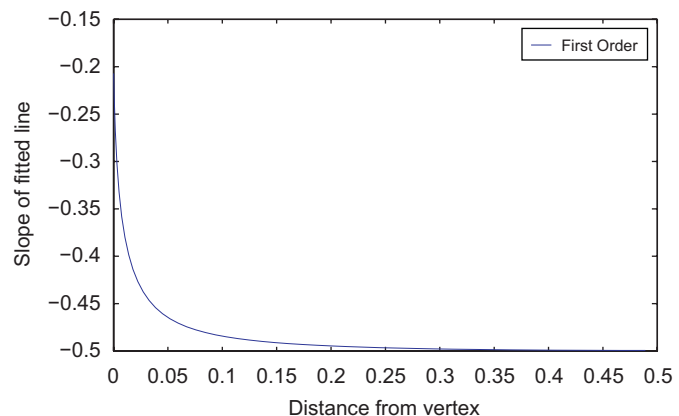mentioned here that in [33,34], the L-shaped volume has been described very nicely in relation to the varying nature of singularities it contains. Capacitance of the L-shaped volume conductor has turned out to be 112.1497 pF. The estimate matches extremely well with the value of 112.15 pF that has been used as a reference value in [33]. In Table 6 we present the numerical values of the order of singularities at inner corners of the L-shaped plate and volume conductor. While the former matches well with [31], the latter is not quite close to the estimate in [33], the difference being close to 20%. Finally, in Fig. 15, we show how the magnitude of charge density changes on a L-shaped plate. The remarkable difference between external and internal corners in terms of charge density concentration is very clearly observed in this figure.

3.2.3. Edge problem having analytical solutions in two dimensions

While none of the above problems have analytic solutions, a closely related problem has well-known analytic solution in the two-dimensional case [29]. In fact, while discussing the earlier problems, other workers and we have quite often referred to this solution obtained in standard textbooks as an exercise in the method of separation of variables.

We have considered a three-dimensional equivalent of the geometry as presented in [29] in which two conducting planes intersect each other at an angle β. The planes are assumed to be held at a given potential. In order to specify the boundary conditions conveniently, a circular cylinder is also included that just encloses the two intersecting plane, has its center at the intersection point and is held at zero potential [48]. The general solution in the polar coordinate system (ρ, ϕ) for the potential (Φ) close to the origin in this problem has been shown to be

$$\Phi(\rho, \phi) = V + \sum_{m=1}^{\infty} a_m \rho^{m\pi/\beta} \sin(m\pi\phi/\beta) \tag{10}$$

where the coefficients a_m depend on the potential remote from the corner at $\rho = 0$ and V represents the boundary condition for Φ for all $\rho \geqslant 0$ when $\phi = 0$ and $\phi = \beta$. In the present case where a circular cylinder just encloses the two plates, the problem of finding out a_m reduces to a basic fourier series problem with a well-known solution

$$a_m = \frac{4}{m\pi} \quad \text{for odd } m \tag{11}$$

Fig. 14. Variation of the slope of the fitted lines along an edge of a square plate.

Table 6
Comparison of estimation of order of singularity

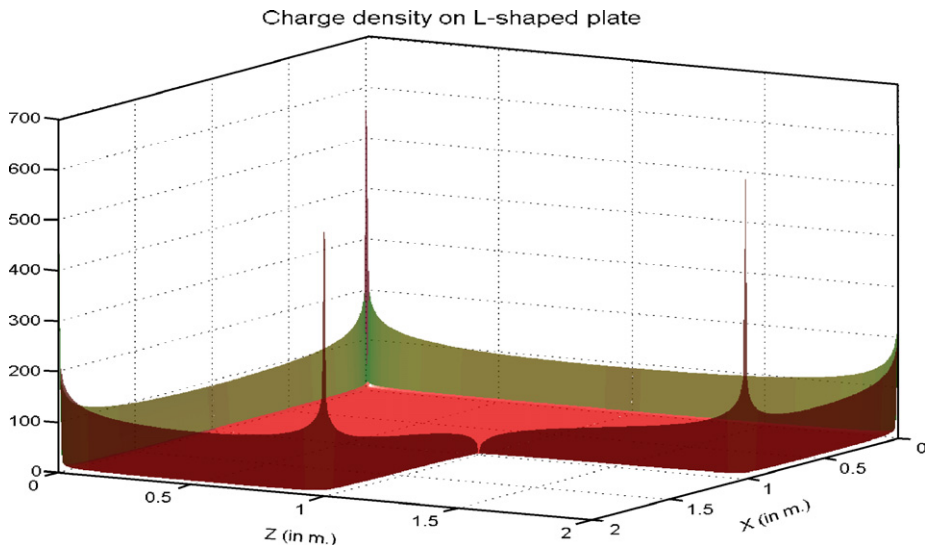| Reference	Method	L Plate inner corner	L volume inner corner
[31]	Numerical shooting	0.1854	
[33]	Singular element		0.1104
This work	neBEM	0.1840	0.0896

Fig. 15. Charge density estimated by neBEM on a L-shaped conducting plate raised to unit volt.

It may be noted here that the series in (10) involve positive powers of $\rho^{\pi/\beta}$, and, thus, close to the origin (i.e., for small ρ), only the first term in the series will be important. The electric field components (E_ρ, E_ϕ) are

$$E_\rho(\rho, \phi) = -\frac{\pi}{\beta} \sum_{m=1}^{\infty} a_m \rho^{(m\pi/\beta)-1} \sin(m\pi\phi/\beta) \qquad (12)$$

$$E_\phi(\rho, \phi) = -\frac{\pi}{\beta} \sum_{m=1}^{\infty} a_m \rho^{(m\pi/\beta)-1} \cos(m\pi\phi/\beta) \qquad (13)$$

The surface charge densities (σ) at $\phi = 0$ and $\phi = \beta$ are equal and are approximately

$$\sigma(\rho) = \frac{E_\phi(\rho, 0)}{4\pi} \simeq -\frac{a_1}{4\beta} \rho^{(\pi/\beta)-1} \qquad (14)$$

Thus, the field components and the charge density near $\rho = 0$ both vary with distance as $\rho^{(\pi/\beta)-1}$ and this fact is expected to be reflected in a correct numerical solution as well.

While the above theoretical solution is a two-dimensional one, we have used the neBEM solver to compute a three-dimensional version of the above problem. In order to reproduce the two-dimensional behavior at the mid-plane, we have made the axial length of the system sufficiently long, viz., 10 times the radius of the cylinder. The radius of the cylinder has been fixed at 1 m, while the length of the intersecting flat plates has been made a mm shorter than the radius to avoid the absurd situation of having two values of the voltage at the same spatial point.

The cylinder has been discretized uniformly in the angular and axial directions. The flat plates have also been uniformly discretized in the axial direction. In the radial direction, however, the flat plate elements have been made successively smaller towards the edges using a simple algebraic equation in order to take care of the fact that the surface charge density increases considerably near the edges. From Tables 7–9, we can compare the accuracy of neBEM results with other analytical and numerical results. The two ends of the range of angles, 360 and 90, represent particularly difficult situations. The former is difficult due to the very large concentration of charge density close to a sharp edge and the resulting large electric field. The latter is difficult due to the fact that to truly simulate a null point in a concave corner, extremely precise estimates are necessary to ensure cancellation of electric field. Throughout the range, the neBEM results are found to be very accurate except at the location that is just 1 μm away from the edge. Even at this location, for all the convex edges, the results are reasonable and surely comparable to the only other numerical result available. The neBEM estimates are unacceptable, however, at locations less than tens of microns away from the null corner of the concave corner. It may be noted, however, that the problem is not at all inherent to the formulation and is clearly related to the size of elements used in the vicinity of the corner. Here, on our desktop PC with 2 GB RAM, we could use a spatial resolution of around a micron close to the corner despite using a large profiling factor. And this was at the steep cost of having elements with extremely large aspect ratios $(1 : 10^6)$. We believe that these are the factors that have resulted in the inaccuracy of the presented results when the locations considered were a micron away from the edge.

To end this section, we present one contour plot of electric field for a convex corner. From Fig. 16, it is evident that the intensity of
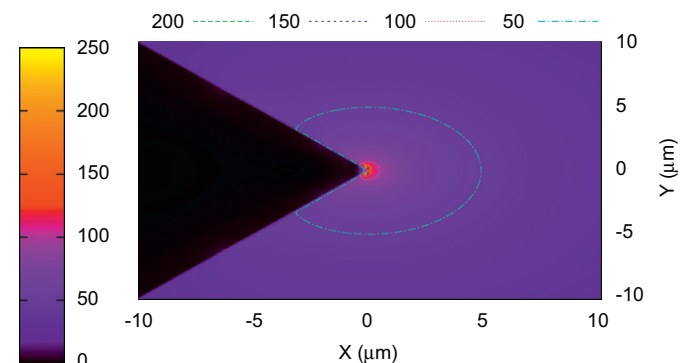
Table 7
Electric field close to a 360° edge

Distance	Analytical	ELECTRO	Error (%)	neBEM	Error (%)
0.8	0.3954180	0.3954213	0.00059	0.3950786	−0.086
0.1	1.830153	1.830155	0.00010	1.830110	−0.002
0.01	6.303166	6.303172	0.000094	6.305784	−0.041
0.001	20.11157	20.11122	0.0018	20.11963	−0.04
0.0001	63.65561	63.64274	0.020	63.64780	−0.012
0.00001	201.3148	200.88	0.22	200.5488	−0.3
0.000001	636.6191	621.25	2.4	621.6034	−2.36

Table 8
Electric field close to a 270° edge

Distance	Analytical	ELECTRO	Error (%)	neBEM	Error (%)
0.8	0.5246997	0.524710	0.0019	0.5241510	−0.105
0.1	1.747623	1.747621	0.00014	1.747953	−0.018
0.01	3.931433	3.931284	0.0038	3.933242	−0.046
0.001	8.487415	8.4854	0.023	8.491335	−0.046
0.0001	18.28732	18.202	0.46	18.29270	−0.029
0.00001	39.39902	35.80	9.1	39.30955	−0.227
0.000001	84.88264	57.10	32.7	80.74309	−4.877

Fig. 16. Electric field distribution very close to a convex edge.

Table 9
Electric field close to 90° and 225° edges

Distance	0.8	0.1	0.01	0.001	0.0001	0.00001	0.000001
	90°						
Analytic	1.445221	2.546224e−1	2.546479e−2	2.546479e−3	2.546479e−4	2.546479e−5	2.546479e−6
neBEM	1.444098	2.547710e−1	2.548018e−2	2.547723e−3	2.778723e−4	3.760117e−3	1.518850
Error (%)	−0.001123	0.058361	0.060436	0.048846	9.120200	usable(?)	inaccurate
	225°						
Analytic	0.6266090	1.574802	2.556973	4.055022	6.426876	10.18592	16.14359
neBEM	0.6259308	1.575165	2.557946	4.056545	6.428439	10.16933	15.63912
Error (%)	−0.108233	−0.023050	−0.038052	−0.037558	−0.024313	−0.162871	−3.124893

the field increases only very close to the convex edge. Note that the dimensions in the figure are mentioned in microns.

4. Conclusion

An efficient and robust library, ISLES, for solving potential problems in a large variety of science and engineering problems has been presented. Exact closed-form expressions used to develop ISLES have been validated throughout the physical domain (including the critical near-field region) by comparing these results with results obtained using numerical quadrature of high accuracy and with those obtained using quadrupole expressions. Algorithmic aspects of this development have also been touched upon. The neBEM solver that uses foundation expressions being evaluated by ISLES has been used to solve several corner and edge electrostatic problems. Several classic benchmark problems such as those related to unit square plate and unit cube have been solved to very high precision. Charge density values at critical geometric locations like corners have been found to be numerically stable and physically acceptable. Values of singularity indices at different corners and edges have been estimated and compared with other analytic and numerical estimates. The agreement among the different approaches has been found to be quite acceptable. It has been observed that the variation of this index along the edge of a conducting body is non-negligible implying caution necessary for methods that need prior knowledge of these indices to solve a given problem. Finally, using the same solver, a three-dimensional equivalent of an edge problem has been solved for which analytic solution exists in two-dimensions. Detail comparison with this problem and those stated earlier have led us to believe that the neBEM approach yields a precise, flexible and robust solver that works over a very wide range of problems. Several advantages over usual BEM solvers and other specialized BEM solvers have been briefly mentioned. Some of the criticisms leveled against the BEM approach in general have been addressed in this work, while we expect to solve some of the remaining in future communications. Work is also under way to make the code more efficient through the implementation of faster algorithms and parallelization.

References

[1] Nagarajan A, Mukherjee S. A mapping method for numerical evaluation of two-dimensional integrals with $1/r$ singularity. Comput Mech 1993;12: 19–26.
[2] Wang J, Tsay T-K. Analytical evaluation and application of the singularities in boundary element method. Eng Anal Boundary Elem 2005;29:241–56.
[3] Cruse TA. Numerical solutions in three dimensional elastostatics. Int J Solids Struct 1969;5:1259–74.
[4] Kutt HR. The numerical evaluation of principal value integrals by finite-part integration. Numer Math 1975;24:205–10.
[5] Lachat JC, Watson JO. Effective numerical treatment of boundary integral equations: a formulation for three dimensional elastostatics. Int J Numer Methods Eng 1976;10:991–1005.
[6] Srivastava R, Contractor DN. Efficient evaluation of integrals in three-dimensional boundary element method using linear shape functions over plane triangular elements. Appl Math Modelling 1992;16:282–90.
[7] Carini A, Salvadori A. Analytical integration in 3D BEM: preliminaries. Comput Mech 2002;18:177–85.
[8] Chyuan S-W, Liao Y-S, Chen J-T. An efficient technique for solving the arbitrarily multilayered electrostatic problems with singularity arising from a degenerate boundary. Semicond Sci Technol 2004;19:R47–58.
[9] Sladek V, Sladek J. Elimination of the boundary layer effect in BEM computation of stresses. Commun Appl Numer Methods 1991;7:539–50.
[10] Mukhopadhyay S, Majumdar N. Computation of 3D MEMS electrostatics using a nearly exact BEM solver. Eng Anal Boundary Elem 2006;30:687–96.
[11] Hess JL, Smith AMO. Calculation of potential flow about arbitrary bodies. Prog Aeronaut Sci 1967;8:1–138.
[12] Newman JN. Distributions of sources and normal dipoles over a quadrilateral panel. J Eng Math 1986;20:113–26.
[13] Goto E, Shi Y, Yoshida N. Extrapolated surface charge method for capacity calculation of polygons and polyhedra. J Comput Phys 1992;100:105–15.
[14] Lazic P, Stefancic H, Abraham H. The Robin Hood method—a novel numerical method for electrostatic problems based on non-local charge transfer. J Comput Phys 2006;213:117–40.
[15] Lazic P, Stefancic H, Abraham H. The Robin Hood method—a new view on differential equations. Eng Anal Boundary Elem 2008;32:76–89.
[16] Bao Z, Mukherjee S. Electrostatic BEM for MEMS with thin conducting plates and shells. Eng Anal Boundary Elem 2004;28:1427–35.
[17] Liao Y-S, Chyuan S-W, Chen J-T. FEM versus BEM. Circuits Devices Mag IEEE 2004;20:25–34.
[18] Mukhopadhyay S, Majumdar N. Effect of finite dimensions on the electric field configuration of cylindrical proportional counters. IEEE Trans Nucl Sci 2006; 53:539–43.
[19] Majumdar N, Mukhopadhyay S. Simulation of three-dimensional electrostatic field configuration in wire chambers: a novel approach. Nucl Instrum Methods Phys Res A 2006;566:489–94.
[20] Mukhopadhyay S, Majumdar N. Use of rectangular and triangular elements for nearly exact BEM solutions. In: Emerging mechanical technology—macro to nano. Chennai, India: Research Publishing Services; 2007. p. 107–14 (ISBN: 81-904262-8-1).
[21] Mukhopadhyay S, Majumdar N. Use of triangular elements for nearly exact BEM solutions, 2007, arXiv:0704.1563.
[22] Majumdar N, Mukhopadhyay S. Simulation of 3D electrostatic configuration in gaseous detectors. J Instrum 2007;2:P09006.
[23] Wintle HJ. The capacitance of the cube and square plate by random walk methods. J Electrostatics 2004;62:51–62.
[24] Maxwell JC, editor. Electrical research of the honorable Henry Cavendish. Cambridge, UK: Cambridge University Press; 1879. p. 426–7.
[25] Maxwell JC. A treatise on electricity and magnetism. Oxford, England: Oxford University Press; 1892.
[26] Reitan DK, Higgins RJ. Accurate determination of capacitance of a thin rectangular plate. Trans AIEE, Part 1 1957;75:761–6.
[27] Read FH. Improved extrapolation technique in the boundary element method to find the capacitance of the unit square and cube. J Comput Phys 1997;133: 1–5.
[28] Read FH. Capacitances and singularities of the unit triangle, square, tetrahedron and cube. COMPEL: the international journal for computation and mathematics in electrical and electronic engineering, vol. 23; 2004. p. 572–8.
[29] Jackson JD. Classical electrodynamics. 2nd ed. New Delhi: Wiley Eastern Limited; 1988.
[30] Smythe WR. Static and dynamic electricity. 3rd ed. New York: Hemisphere; 1989.
[31] Morrison JA, Lewis JA. Charge singularity at the corner of a flat plate. SIAM J Appl Math 1976;31:233–50.
[32] Greenfield D, Monastyrski M. Three dimensional electrostatic field calculation with effective algorithm of surface charge singularities treatment based on the Fichera's theorem. Nucl Instrum Methods Phys Res Sect A Acceler Spectrometers Detectors Assoc Equip 2004;519:82–9.
[33] Ong ET, Lim KM. Three-dimensional singular boundary elements for corner and edge singularities in potential problems. Eng Anal Boundary Elem 2005;29:175–89.
[34] Su Y, Ong ET, Lee KH. Automatic classification of singular elements for the electrostatic analysis of microelectromechanical systems. J Micromech Microeng 2002;12:307–15.
[35] ⟨http://www.msc.com⟩.
[36] Bazant ZP. Three-dimensional harmonic functions near termination or intersection of gradient singularity lines: a general numerical method. Int J Eng Sci 1974;12:221–43.
[37] Aiza MP, Saez A, Dominniguez JA. A singular element for three-dimensional fracture mechanics analysis. Eng Anal Boundary Elem 1997;20: 275–85.
[38] El Abdi R, Valentin G. Isoparametric elements for a crack normal to the interface between two bonded layers. Comput Struct 1989;33:241–8.
[39] Jun Q, Norio H. On the technique of shifting side-nodes in isoparametric elements to impose arbitrary singularity. Comput Struct 1998;66:841–6.
[40] Zhou H-X, Szabo A, Douglas JF, Hubbard JB. A Brownian dynamics algorithm for calculating the hydrodynamic friction and the electrostatic capacitance of an arbitrarily shaped object. J Chem Phys 1994;100:3821–6.
[41] Given JA, Hubbard JB, Douglas JF. A first-passage algorithm for the hydrodynamic friction and diffusion-limited reaction rate of macromolecules. J Chem Phys 1997;106(9):3721–71.
[42] Hwang C-O, Given JA, Mascagni M. The simulation-tabulation method for classical diffusion Monte Carlo. J Comput Phys 2001;174:925–48.

[43] Mansfield ML, Douglas JF, Garboczi EJ. Intrinsic viscosity and the electrical polarizability of arbitrarily shaped objects. Phys Rev E 2001;64(6): 061401–16.

[44] Given JA, Hwang C-O. Edge distribution method for solving elliptic boundary value problems with boundary singularities. Phys Rev E 2003;68. 046128-1–6.

[45] Mascagni M, Simonov NA. The random walk on the boundary method for calculating capacitance. J Comput Phys 2004;195(2):465–73.

[46] Hwang C-O, Won T. Last-passage algorithms for corner charge singularity of conductors. J Korean Phys Soc 2005;47:S464–6.

[47] Sato S. Effective three-dimensional electric field analysis by surface charge simulation method. Dissertation, ETH Zurich; 1987.

[48] ⟨http://www.integratedsoft.com/papers/benchmark/corner⟩.

[49] Etter DM. Engineering problem solving with MatLab. Englewood Cliffs, NJ, USA: Prentice-Hall; 1997.

[50] Greengard L, Rokhlin V. A fast algorithm for particle simulation. J Comput Phys 1987;73:325–48.

[51] Saad Y, Schultz M. GMRES: a generalized minimal residual algorithm for solving nonsymmetric linear systems. SIAM J Sci Statist Comput 1986;7: 856–69.

[52] Solomon L. C R Acad Sci III 1964;258:64.

[53] Schimtz H, Volk K, Wendlandt W. Three-dimensional singularities of elastic fields near vertices. Numer Methods Partial Differential Equation 1993;9: 323–37.